



**HAL**  
open science

## Two SCA (Stigma/Style Cysteine-rich Adhesin) Isoforms Show Structural Differences That Correlate with Their Levels of in Vitro Pollen Tube Adhesion Activity

Keun Chae, Kangling Zhang, Li Zhang, Dimitrios Morikis, Sun Tae Kim, Jean-Claude Mollet, Noelle de La Rosa, Kimberly Tan, Elizabeth M Lord

### ► To cite this version:

Keun Chae, Kangling Zhang, Li Zhang, Dimitrios Morikis, Sun Tae Kim, et al.. Two SCA (Stigma/Style Cysteine-rich Adhesin) Isoforms Show Structural Differences That Correlate with Their Levels of in Vitro Pollen Tube Adhesion Activity. *Journal of Biological Chemistry*, 2007, 282 (46), pp.33845-33858. 10.1074/jbc.M703997200 . hal-02121409

**HAL Id: hal-02121409**

**<https://normandie-univ.hal.science/hal-02121409>**

Submitted on 6 May 2019

**HAL** is a multi-disciplinary open access archive for the deposit and dissemination of scientific research documents, whether they are published or not. The documents may come from teaching and research institutions in France or abroad, or from public or private research centers.

L'archive ouverte pluridisciplinaire **HAL**, est destinée au dépôt et à la diffusion de documents scientifiques de niveau recherche, publiés ou non, émanant des établissements d'enseignement et de recherche français ou étrangers, des laboratoires publics ou privés.

## Two SCA (Stigma/style Cysteine-rich Adhesin) isoforms show structural differences that correlate with their levels of *in vitro* pollen tube adhesion activity.

Keun Chae<sup>1,2</sup>, Kangling Zhang<sup>3</sup>, Li Zhang<sup>4</sup>, Dimitrios Morikis<sup>5</sup>, Sun Tae Kim<sup>6</sup>, Jean-Claude Mollet<sup>7</sup>,  
Noelle de la Rosa<sup>2</sup>, Kimberly Tan<sup>2</sup>, Elizabeth M. Lord<sup>1,2</sup>

From <sup>1</sup>Center for Plant Cell Biology, <sup>2</sup>Department of Botany and Plant Sciences, <sup>3</sup>Mass Spectrometry Facility, <sup>4</sup>Department of Chemistry, <sup>5</sup>Department of Bioengineering, University of California, Riverside, CA 92521, USA, <sup>6</sup>Environmental Biotechnology National Core Research Center, Gyeongsang National University, Jinju 660-701, Korea, <sup>7</sup>Laboratoire de Glycobiologie et Transports chez les Végétaux, UMR CNRS 6037, IRFPM 23, Université de Rouen, 76821 Mont Saint-Aignan Cedex, France

Running title: Pollen tube adhesion activity of lily SCA isoforms

Address correspondence to: Elizabeth M. Lord, Center for Plant Cell Biology, Department of Botany and Plant Sciences, University of California, Riverside, CA 92521, USA, Tel: 1-951-827-4441, Fax: 1-951-827-4437, E-mail: [lord@ucr.edu](mailto:lord@ucr.edu)

Lily pollen tubes grow adhering to an extracellular matrix (ECM) produced by the transmitting tract epidermis in a hollow style. SCA, a small (~ 9.4 kDa), basic protein, plus low-esterified pectin from this ECM are involved in the pollen tube adhesion event. The mode of action for this adhesion event is unknown. We partially separated three SCA isoforms from the lily stigma in serial size-exclusion column fractions (SCA1: 9370 Da, SCA2: 9384 Da, SCA3: 9484 Da). Peptide sequencing analysis allowed us to determine two amino acid variations in SCA3, compared to SCA1. For SCA2, however, there are more sequence variations yet to be identified. Our structural homology and molecular dynamics (MD) modeling results show that SCA isoforms have the plant non-specific lipid transfer protein (nsLTP)-like structure: a globular shape of the orthogonal 4-helix bundle architecture, four disulfide bonds, an internal hydrophobic and solvent inaccessible cavity, and a long C-terminal tail. The Ala71 in SCA3, replacing the Gly71 in SCA1, has no predictable effect on structure. The Arg26 in SCA3, replacing the Gly26 in SCA1, is predicted to cause structural changes that result in a significantly reduced volume for the internal hydrophobic cavity in SCA3. The volume of the internal cavity fluctuates slightly during the MD simulation, but overall, SCA1 displays a larger cavity than SCA3. SCA1 displays higher activity than SCA3 in the *in vitro* pollen tube adhesion assay. No differences

were found between the two SCAs in a binding assay with pectin. The larger size of the hydrophobic cavity in SCA1 correlates with its higher adhesion activity.

During lily pollination, pollen tubes are guided to the ovary on an extracellular matrix (ECM) produced by the specialized stylar transmitting tract epidermis (TTE). This guidance includes an adhesion event between the pollen tube and the TTE (1-4). For the purpose of identifying molecular factors in lily pollen tube adhesion, Jauh et al (5) developed an *in vitro* bioassay using ECM molecules attached to a nitrocellulose membrane as an artificial style. Using this *in vitro* bioassay, two molecules from the style ECM, SCA (Stigma/style Cysteine-rich Adhesin) and a low esterified pectic polysaccharide, were found to be responsible for pollen tube adhesion on the stylar matrix (6,7). The level of SCA mRNA was high in stigma/style tissue, petal and young leaf, but it was absent in pollen tubes (8). Localization of both SCA and the low-esterified pectin on the surface of the stylar TTE supported their involvement in *in vivo* pollen tube adhesion. The mechanism of action for SCA and pectin in pollen tube adhesion is yet unknown. Neither of these molecules alone is active in the adhesion assay. Only when they were combined, do SCA and pectin bind to each other in a pH-dependent manner and form the functional, adhesive matrix (6). The pH effect implies that a charge interaction occurs, rather than a tight cross-linking, between SCA and the low esterified pectin in lily pistils.

SCA is a small (~ 9.4 kDa), basic protein (pI: ~ 9.0) with around 50% amino acid sequence homology to plant non-specific lipid transfer proteins (nsLTPs) (7). Plant nsLTPs are small (9 – 10 kDa) in size, basic (pI: 8.8 – 10) proteins (9,10). They were named LTPs because of a presumed intracellular function in transport of lipids between organelles. The three-dimensional structures of several known plant nsLTPs show a globular molecule, composed of four  $\alpha$ -helices, which are stabilized by four disulfide bridges, and a C-terminal tail (11-13). The most outstanding feature of this hydrophilic molecule is a hydrophobic cavity that runs through the whole molecule and, in several known cases, is capable of interacting with the acyl-chain of a phospholipid molecule and fatty acids (14,15). Plant nsLTPs appear to have no specificity for binding lipids, and they even bind two mono-acylated lipid monomers (16-18) or a diacylated lipid (19). Although many LTPs can bind lipids *in vitro*, no LTP has been shown to do so *in vivo*. In addition, plant nsLTP family members contain an N-terminal signal peptide that makes mature proteins enter the secretory pathway and be present in the extracellular space (20,21). So, the early assumption that they function intracellularly in lipid transfer is now discredited and a function in the extracellular matrix or wall is sought.

Except for a few cases, the biological functions of plant nsLTPs are unknown. Some LTPs have been shown to have potent antimicrobial (22) or antifungal activity (23). A putative lipid transfer protein, DIR-1, was recently shown to be involved in systemic resistance in Arabidopsis (24). A tobacco LTP was shown to mediate cell wall-loosening *in vitro* (25). In our work, SCA, a lily LTP, has been shown to act with pectin in forming an adhesive stigma/stylar matrix for pollen tube guidance (6,7).

Low molecular weight (7 – 10 kDa) lily stigma protein fractions (stigma proteins, SPs), were previously prepared using ion exchange and size exclusion chromatography (7,26). The major peak found in the HPLC profile of the SPs was identified as SCA (HPLC-SCA) (26). The theoretical mass of SCA was calculated as 9371 Da, with eight-cysteine residues in an oxidized status, based upon deduced peptide sequences from a previously cloned SCA cDNA from the lily stigma (7). The ESI-MS analysis showed that the

HPLC-SCA peak contained major masses of 9369.5 Da and 9385.3 Da (MSO: methionine oxidized form of SCA with a 16 Da-mass increase). However, there were two other SCA-like masses also present in the HPLC-SCA peaks (9384 Da and 9484 Da) (26). In addition to the three putative SCA isoforms identified, several other proteins with masses ranging between 5170 and 9898 Da were also found in the SPs. Among them, a small peak was identified as chemocyanin (9.8 kDa), another secreted protein in the lily stigma that functions in pollen tube guidance (26).

Although we have identified putative isoforms of SCA present in the lily stigma, we were not able to proceed further to identify their sequence differences from the originally sequenced SCA, nor to do functional analysis of the isoforms using our adhesion assay. This was due to difficulties in separating the HPLC-SCA peaks. In the current study, we succeeded in partially separating SCA isoforms from the lily stigma using size-exclusion chromatography and identifying them using ESI-MS analysis, following HPLC purification. Following the partial separation of isoforms, ESI-MS/MS analysis with trypsin-digestion helped us to verify the amino acid differences among the isoforms. We were able to determine the primary sequence for SCA3, but we achieved complete sequences for only a signature peptide from SCA2. Complete sequencing of SCA2 remains to be accomplished. We used computational analyses to generate homology/MD structures for the two sequenced SCA isoforms (SCA1 and SCA3), demonstrating that one amino acid change can cause a significant structural change in the molecule, especially in the size of the internal hydrophobic cavity. This difference in structure correlates with a difference in activity of the two isoforms in the *in vitro* pollen tube adhesion assay. The significance of the structural change is discussed in light of our recent studies on the interaction between SCA and the pollen tube (27).

## Materials and Methods

*Plant materials* – *Lilium longiflorum* Thunb. plants (cvs. Nellie White and Snow Queen) were grown in the green house at the University of California, Riverside. Stigmas were collected within 5 days after anthesis and stored at – 80°C until used for protein preparation. For *in vitro*

adhesion assays, fresh pollen was used from anthers at 2 – 3 days after anthesis.

*Preparation of lily stigma proteins* – The protein purification was done by the method previously described (26), with a few modifications. Briefly, 64 g of frozen stigmas were ground in PBS (0.14 M NaCl, 2.7 mM KCl, 1.5 mM KH<sub>2</sub>PO<sub>4</sub>, and 8.1 mM Na<sub>2</sub>HPO<sub>4</sub>, pH 7.4), and proteins were precipitated with a stepwise gradient of (NH<sub>4</sub>)<sub>2</sub>SO<sub>4</sub> (25 – 90%). All precipitates were pooled and dialyzed against ddH<sub>2</sub>O (MilliQ, Millipore). The proteins were applied to a CM-Sephadex C-25 cation exchange column (20mM MES buffer/pH 5.6) and serially eluted with 0.1, 0.5, 0.75, and 1 M NaCl in 20mM MES buffer. The fractions containing SCA were identified by western blots and further fractionated on an Acrylamide Bio-gel P10 column (120 × 1 cm, Bio-Rad). We refer to these size column fractions as stigma proteins (SPs), which mainly contain SCA (over 90%), with some other small, extracellular proteins.

The crude stigma proteins were obtained from a single stigma of either Nellie White or Snow Queen at 3 days after anthesis. Fresh stigma tissue was ground in PBS buffer (0.14 M NaCl, 2.7 mM KCl, 1.5 mM KH<sub>2</sub>PO<sub>4</sub>, and 8.1 mM Na<sub>2</sub>HPO<sub>4</sub>, pH 7.4). Larger-sized molecules were excluded by a precipitation with 70% Methanol. The supernatant solution, containing relatively small-sized molecules, was incubated with CM-Sephadex C-25 beads in 20mM MES buffer/pH 5.6 at 4°C for 30 minutes. Any unbound proteins were washed from the resins with 20mM MES buffer/pH 5.6, and the bound proteins were eluted using 0.5M NaCl. After dialysis against ddH<sub>2</sub>O, crude stigma protein samples were subjected to ESI-MS analysis.

*HPLC purification of SCA* – SPs were further purified by HPLC (Agilent 1100, Hewlett-Packard) with a Jupiter C4 microbore column (2 × 250 mm, 5-μm particle diameter, 100-Å pore size, Phenomenex, Belmont, CA) to obtain pure SCA proteins (referred to as HPLC-SCAs). SPs (~50 μg), dissolved in water, were injected into the HPLC column, and proteins were eluted with a two-step linear gradient at a flow rate of 50 μl/min from a 5% mobile phase B (0.1% trifluoroacetic acid in CH<sub>3</sub>CN) to a 45% B for 30 min, holding at 45% B for 5 min, and then ramping to 90% B for another 50 min. The peaks corresponding to SCA

were collected, evaporated, and then re-dissolved in 0.1% formic acid in an appropriate volume of ACN/H<sub>2</sub>O (50:50 v/v) for mass spectrometric analysis of protein molecular weight. In addition, an aliquot of the fractions was dissolved in 25 mM ammonium bi-carbonate for enzymatic digestion and applied to mass spectrometric sequence analysis. HPLC-SCAs were used for production of polyclonal SCA antibodies as well as for all *in vitro* bioassays and mass spectrometry in this study.

*Purification of low-esterified pectins from the lily style* – Lily stylar pectins, used for all *in vitro* bioassays, were prepared by following the previously established method (6). Briefly, fresh lily styles were cut into 1.5 cm segments and then cut in half lengthwise to expose the transmitting tract epidermis (TTE). The style segments were continuously stirred for 30 min at 70°C with PAW reagent (250 ml of 80% phenol and 100 ml of acetic acid). The extract was filtered through a Büchner funnel (w/ filter paper) and discarded. The style fragments were recovered and rinsed serially with ddH<sub>2</sub>O, 95% EtOH, and ddH<sub>2</sub>O. The style segments were continuously stirred for 16 hr at room temperature in 500mM Imidazole-HCl/pH7.0 (0.02% NaN<sub>3</sub>) buffer. The extract was filtered and saved for a centrifugation at 4,000 rpm for 30 min at 4°C. The supernatant was dialyzed against ddH<sub>2</sub>O and added to Imidazole-HCl/pH7.0 buffer for a final concentration of 100mM. The sample was then applied to an anion-exchange column (Q-Sepharose) and eluted with a serial Imidazole gradient (250mM, 500mM, 1M, and 1.5M). The elute, which was active in the *in vitro* bioassay, was further fractionated using a size-exclusion column (Sepharose CL-6B). All fractions collected were applied for phenol sulfuric (28) and meta-hydroxybiphenyl (29) assays to determine carbohydrate profile. The adhesive fractions were pooled. After dialysis against ddH<sub>2</sub>O and freeze-dry concentration, the 1ml-aliquots of low-esterified pectin samples were kept at –20°C, until used for the bioassay.

*In vitro pollen tube adhesion assay* – The pollen tube adhesion assay followed a previous method with a few modifications (7). HPLC-purified SCA proteins were vacuum-dried and re-dissolved in water. 10μg of proteins, determined by the Lowry Modified Protein Assay (Pierce Biotechnology

Inc.), were combined with 40 $\mu$ g of lily stylar pectin. SCA-Pectin mixtures were incubated at room temperature for 15 minutes and transferred onto nitrocellulose using a dot-blotter with six 0.8mm-diameter wells. The nitrocellulose membranes were air-dried, and pre-germinated pollen tubes (2 – 3 hours) in germination medium were laid on top of the SCA-pectin matrix in a petri dish and incubated at room temperature in the dark for an additional 5 hours without any disturbance. The membranes were gently washed with germination medium, stained with Coomassie brilliant blue R-250, and the number of bound pollen tubes was counted under a dissecting microscope.

*In vitro pectin binding assay* – 5 $\mu$ g of HPLC-SCA was incubated with 40 $\mu$ g of stylar pectins at room temperature for 30min in a total 100 $\mu$ l of reaction volume. A 10 $\mu$ l aliquot from each reaction sample was saved as a loading control and 90 $\mu$ l of the SCA-pectin mixture was applied to the 100-kD cut-off spin-column (Microcon, Millipore Co.). Any proteins released from the pectin matrix were passed through the column by centrifugation at 3,000 rpm for 10 min. Proteins that were tightly bound to pectins (retentates) and left over on top of the column were recovered by 90 $\mu$ l of ddH<sub>2</sub>O. To ensure 100% recovery of the retentates, 90 $\mu$ l of 1M NaCl was used for the final elution (elutes). 10 $\mu$ l of aliquots from the control, retentates and elutes were applied to SDS-PAGE, and the amount of pectin-binding SCA was evaluated in western blots using SCA-antibodies.

To determine what ionic strength is required for SCA's interaction with pectin, Bio-gel P10 size-column fractions 28 (SCA1-enriched SPs) and 31 (SCA3-enriched SPs) were mixed with stylar pectins, respectively. After a 30min-incubation at room temperature, each SCA-pectin mixture was loaded on top of the 100-kD cut-off spin-column. Elutions were repeated using each NaCl (from 0 to 1000 mM) to determine at which ionic strength SCA proteins are eluted from the pectin matrices. The retentate after the final elution was also recovered by 90 $\mu$ l of ddH<sub>2</sub>O to ensure that there is no protein left over on the pectin matrix. All serial elutes were applied to SDS-PAGE and SCA proteins that detached from the pectin matrix at a certain ionic strength were detected using western blots.

*Production of polyclonal antibodies and western blotting* – Highly specific antibodies against pure SCA were generated by an injection of HPLC-SCA into rabbits (Cocalico Biologicals Inc.). Chemocyanin antibodies were made against the recombinant His-tagged protein (30). Both antibodies have high specificity to each protein without showing any cross-reactivity (Fig. S1). Among several fractions of SPs obtained through ion- and size-columns, SCA-enriched fractions were identified by western blotting using polyclonal SCA antibodies. Proteins, dissolved in H<sub>2</sub>O, were combined with an equal volume of 2 $\times$ SDS sample buffer (125 mM Tris-HCl/pH 6.8, 4% [v/v] SDS, 20% [v/v] glycerol, 0.01% [w/v] bromophenol blue, and 10mM DTT), boiled at 95 $^{\circ}$ C for 5 min, and separated by 15% SDS-PAGE. Proteins were then transferred to nitrocellulose membrane by electroblotting. Nonspecific antibody interactions were pre-blocked by 5% (w/v) dry-milk powder in Tris-buffered saline plus Tween 20 (20 mM Tris-HCl and 0.2 M sodium chloride at pH 7.6 with 0.1% [v/v] Tween 20). The membrane was treated with 1:1,000 dilutions of the primary antibodies. The signal was detected with secondary goat anti-rabbit antibodies conjugated with a horseradish peroxidase (Bio-Rad) using the Chemiluminescence Reagent Plus (Bio-Rad).

*ESI-MS analysis of HPLC-purified SCAs* – Molecular weight of intact proteins was measured by nanoelectrospray ionization ion source by using a quadrupole-time-of-flight Ultima-global mass spectrometer (Waters, Manchester, UK). About 5  $\mu$ l of proteins purified from HPLC were loaded into the nanoelectrospray tip (Protana, Odense, Denmark) for ESI-MS analysis. The acquired spectra were further processed using the MAXENT\_1 deconvolution software within the instrument control software MASSLYNX to reconstruct the multiple charged ion mass spectra to the singly charged ion mass spectra for the observation of the mono-isotopic mass of proteins. Relative quantification of SCA isoforms was determined through the mono-isotopic peak ratio of the post-deconvolution spectra corresponding to the SCA isoforms.

*Peptide sequence analysis by LC-MS/MS* – SCA fractions collected from HPLC were dissolved in 20  $\mu$ l of 25 mM NH<sub>4</sub>HCO<sub>3</sub>. After reduction of

cysteine residues by incubation with 25  $\mu$ l of 10 mM DTT for 45 min at 57 °C and alkylation by reaction with 25  $\mu$ l of 55 mM iodoacetamide in the dark for an hour, proteins were digested with trypsin (modified sequencing grade, Roche Molecular Biochemicals) at 37 °C over-night, dried, redissolved in 10  $\mu$ l of water, and injected into an HPLC column for LC-MS/MS analysis. The LC-MS/MS experiments were performed on an HP 1100 capillary HPLC (Hewlett-Packard, Palo Alto, CA, USA) using a 0.3 x 150 mm column (Zorbax SB-C18, 5  $\mu$ m, Agilent, Palo Alto, CA, USA) at a flow rate of 6  $\mu$ l/min with multiple steps of a gradient from 2% to 90% mobile phase B over 100 min. Mobile phase B is 0.1 % (v/v) formic acid in H<sub>2</sub>O. Mobile phase B was 0.1 % (v/v) formic acid in acetonitrile. The HPLC was connected on-line to a Waters hybrid quadrupole-time of flight (Q-TOF) mass spectrometer (Waters, Manchester, UK). The Q-TOF method utilized consisted of a survey scan mode in the mass range from 300 to 1400 during which up to four precursor ions were selected for parallel collision dissociation (CAD) analysis using an automated data-dependent switching function; either MS to MS/MS or MS/MS to MS. Precursor ions were fragmented using an *m/z* dependent collision energy applied linearly from 20 to 42 V from 300 to 1400 *m/z* (optimized for doubly charged ions). Product ion scans were measured in the range from *m/z* 50 to 1900. Fragmented peptides were manually analyzed to determine the peptide sequences (*De novo* sequencing).

**MALDI-TOF mass spectrometry** – A 0.5  $\mu$ l aliquot of the trypsin digest of each HPLC-purified SCA fraction was mixed with 0.5  $\mu$ l  $\alpha$ -cyano-4-hydroxycinnamide acid matrix (Sigma, St. Louis, MO) and subjected to MALDI analysis. Mono-isotopic *m/z* values of all peptides were measured by MALDI using a Voyager DE-STR Biospectrometry Workstation (ABI, Palo Alto) with delayed extraction operated in the reflectron mode.

**Computational studies** – Structural homology modeling for SCA1 and SCA3 was performed using the SWISS-MODEL web server (<http://swissmodel.expasy.org>) (31). Several structures of plant nonspecific lipid-transfer protein (LTP) from Protein Data Bank (PDB) (32) were used as structural homology templates: four

maize LTPs (PDB codes 1fk4A, 1fk1A, 1fk0A, and 1fk5A) (33) and one mung bean LTP1 (PDB code 1siyA) (34) for SCA1; three maize LTPs (PDB codes 1fk6A, 1fk4A, and 1mzm) (11,33), one mung bean LTP1 (PDB code 1siyA) (34), and one tobacco LTP (PDB code 1t12A) (35) for SCA3. The high sequence identity between SCA proteins and these plant nsLTPs (38%-58%, Fig. 4) allowed us to perform homology modeling to predict their structures. It is generally accepted that sequence identity at 40% or higher, allows for the prediction of the structural motif of an unknown structure with high confidence (36). The presence of four disulfide bonds further boosts our confidence for the correctness of the structural motif. The disulfide bonds restrict the flexibility of SCAs, and nsLTPs in general, and, together with the hydrophobic core, contribute to enhanced protein stability. Nevertheless, we deemed it necessary to perform short-time molecular dynamics simulations to further relax the predicted structures and to optimize the backbone and side chain conformations and the relative topologies of elements of secondary structure.

Molecular dynamics simulations (37) were performed using the program CHARMM (38), version 31b1. The initial structures were the structural homology models for SCA1 and SCA3 and the crystallographic structure of maize LTP (PDB Code 1mzl)(11). The three proteins possess ~56% sequence identity. The generalized Born implicit solvation energy module (39) and the CHARMM 19 parameter set were used, as implemented within CHARMM 31b1. The electrostatic and van der Waals cutoff was set to 16Å with a switching function between 10 and 14Å. The SHAKE algorithm (40) was used to fix the length of covalent bonds of hydrogen atoms. The time step was set to 2fs. The structure was first energy minimized for 300 steps using the adopted-basis Newton-Raphson (ABNR) method. Then, the structure was subjected to 5ps of MD simulation, during which time the temperature was raised from 0K to 298K with velocity rescaled every 0.1ps. At 298K, a 30ps equilibration phase was initiated with velocity being rescaled only if the temperature deviated more than 5K from 298K. After the equilibration, a 1ns MD trajectory was generated at 298K. Coordinate sets were sampled every 10ps to generate 100 snapshots of structures during the MD trajectory. For our analysis

presented here, we chose the 200ps MD structures of SCA1, SCA3, and Maize LTP. The goal of the molecular dynamics simulation was to generate relaxed structures with optimized potential energies, rather than exploring the conformational space of SCAs. The 200ps MD structures were sufficient for this purpose.

Electrostatic calculations (41) were performed using the program UHBD version 5.1 (42). The finite difference Poisson-Boltzmann solver of UHBD was used to calculate electrostatic potentials with the linearized form of the Poisson-Boltzmann equation and continuum solvent representation. The input structures were the 200ns structural snapshots from the MD simulations for SCA1 and SCA3 and the crystallographic structure of maize LTP (11). Apparent  $pK_a$  and protein stability calculations were performed using the combined method of Antosiewicz et al. (43) and Gilson (44), with the programs UHBD and HYBRID. The dielectric coefficients were set to 78.4 and 20 for the solvent and protein interior, respectively. The temperature was set to 298 K and the ionic strength was set to 0 mM or 50 mM salt concentration. For the parameter set of charges and van der Waals radii, PARSE (45) was used. The molecular surface was defined with a solvent probe of 1.4Å radius and the ion-exclusion layer was defined using a probe of 2.0Å radius. Sequential focusing cubic grids were used with the following dimensions – spacings:  $64 \times 64 \times 64 - 4.0\text{Å}$ ,  $50 \times 50 \times 50 - 2.5\text{Å}$ ,  $30 \times 30 \times 30 - 1.25\text{Å}$ ,  $25 \times 25 \times 25 - 0.5\text{Å}$ , and  $20 \times 20 \times 20 - 0.25\text{Å}$ .

The pH-dependence of protein stability is proportional to the difference between the ionization free energies of the folded and unfolded protein states,  $\Delta\Delta G^{\text{ion}} = \Delta G^{\text{ion, folded}} - \Delta G^{\text{ion, unfolded}}$  (41). Indeed, the stability plots presented hereafter are the  $\Delta\Delta G^{\text{ion}} - \text{pH}$  profiles, which upon proper scaling (usually to match experimental data, if available) are equivalent to  $\Delta G^{\text{stability}}$ ; the quantity  $\Delta G^{\text{stability}}$  being the difference in the free energies of the folded and unfolded protein states in the unfolded  $\rightarrow$  folded protein transition (41). For this reason, only comparative studies for  $\Delta G^{\text{stability}}$  are meaningful, since the scaling factors for the folded and unfolded states are in principle different. We refer to comparative studies of the SCA isoforms at different pHs and two ionic strengths (0 mM

and 50 mM NaCl). The ionization free energies,  $\Delta G^{\text{ion, unfolded}}$  and  $\Delta G^{\text{ion, folded}}$ , which are absolute values, were calculated using the formalism of Yang et al. (46) and the clustering method of Gilson (44).

Structural analysis and generation of molecular graphics were performed using the program Swiss-PDB Viewer (47) and MOLMOL (48). Electrostatic potential calculations for the generation of isopotential contour plots were performed using the program GRASP (49) with the PARSE parameter set, in the absence of salt and in the presence of 50mM salt. For GRASP calculations, the dielectric coefficients were set to 78.5 and 4 for the solvent and protein, respectively. The temperature was set to 298K.

## RESULTS

*Three SCA isoforms were purified from the lily stigma with a partial separation.*

Use of size-exclusion chromatography enabled a partial separation of the three SCA isoforms (Fig. 1). We used Bio-gel P10 resin for the column, which provided us with the resolution to separate small sized-molecules, compared to the previously used sephadex G-50 column (26). Among the fractions serially collected from the size-column, fractions 21 to 32 were shown to contain SCA proteins. Chemocyanin, a small protein that previously was purified with SCA (26), was nearly separated from SCA proteins.

In order to obtain pure SCA proteins, about 55  $\mu\text{g}$  from each size-column fraction (from 21 to 31, respectively) was applied to HPLC (Fig. 2A). The peaks, corresponding to SCA protein in the HPLC profile, were collected and examined for mass composition using ESI-MS (Fig. 2 and Fig. S2). Two additional putative SCA isoforms (26) were also found throughout the fractions. One is 9384 Da, about 14 Da larger than the mass of SCA. Here we name this protein SCA2, while we rename the original one (7) as SCA1 (9370 Da). The other SCA-like mass is 9484 Da, which is 114 Da larger than that of SCA1, and we name it SCA3. In fraction 24, there were three major peptides found at  $m/z$  9370, 9385, and 9401 (Fig. 2B). The ion peak at  $m/z$  9370 indicates the molecular mass (Da) of SCA1. The highest peak at  $m/z$  9385 can represent the mass of either SCA1 containing a methionine sulfoxide (SCA1-MSO:

9386 Da) or SCA2 (9384 Da). Based upon the abundance of the peak at  $m/z$  9401 (SCA2-MSO), we presume that significant amounts of SCA2 are also present in this fraction. In fraction 27, SCA1 (9370 Da) was almost exclusively present but a noticeable SCA2 peak at  $m/z$  9401 was not found (Fig. 2C). In fraction 30, SCA1 levels became greatly reduced while SCA3 (9484 Da) and SCA3-MSO (9500 Da) were highly enriched (Fig. 2D). Taken together, we were able to obtain three fractions which clearly showed unique abundances of SCA isoforms: SCA1 and SCA2 in fraction 24, SCA1 in fraction 27, and SCA3 in fraction 30, although SCA isoforms were not separated with 100% purity.

In ESI-MS profiles of the crude stigma protein prep (see materials and methods), SCA1 was found to be the most abundant amongst three SCA isoforms in the lily stigma (Fig. 2E). This abundance pattern was not variety-specific in *Lilium longiflorum* plants. SCA1 is the major isoform in stigmas of both Nellie White and Snow Queen, varieties of *L. longiflorum* (data not shown).

*Three novel SCA peptide sequences were found and assigned to each SCA isoform.*

To determine amino acid sequences of SCA isoforms, we subjected the HPLC-purified sephadex G-50 size-column fraction of SCA to ESI-MS/MS analysis after trypsin digestion. All peptide fragments that belong to SCA1 were identified (Table 1), and three new peptide fragments were also found (Table 1, underlined sequences: P4, P9, and P11). The first new peptide P4 [20-GGVIPPR-26, 695.4 Da] contained Arg26 (bold letter) instead of Gly26 for SCA1 shown in P2 and P3. The second new peptide P9 [53-SLVNPSLGLNAAIVAGIPAK-72, 1905.1 Da] showed one amino acid change compared to its SCA1 counterpart P10 [53-SLVNPSLGLNAAIVAGIPGK-72, 1891.1 Da]; Ala71 replaces Gly71 (bold letters), resulting in a mass increase of 14 Da. The third new peptide P11 [59-LGLNPAIVAGGIPK-72, 1319.8 Da] showed some more variations (bold letters) in amino acid sequence compared to SCA1 sequences; Pro63 instead of Ala63, and [69-GIP-71] instead of [69-IPG-71].

For correct assignment of the three new peptides into SCA2 or SCA3, we repeated the

peptide sequence analysis using HPLC-purified Bio-gel P10 fractions, where SCA isoforms were partially separated, as shown in Figure 2. First, we evaluated mass abundances of the new peptides P9 and P11 (Fig. 3). The peptide P10 [53-SLVNPSLGLNAAIVAGIPGK-72, 1891.1 Da] was previously identified as the SCA1 sequence by deduction from the cDNA (7). Its doubly charged ion at  $m/z$  946.04 showed the highest abundance in fraction 27 (Fig. 3B), but it was significantly decreased in fraction 30 (Fig. 3C). This pattern is well matched with the mass abundance of SCA1 shown in Figure 2. The ion mass at  $m/z$  953.04, the doubly charged peptide P9 [53-SLVNPSLGLNAAIVAGIPAK-72, 1905.12 Da], was found most abundantly in fraction 30 (Fig. 3C), in which SCA3 was identified as the most abundant isoform (Fig. 2D). Therefore, this peptide was assigned to SCA3. ESI-MS/MS analysis from the nearly complete set of C-terminal (y) and N-terminal (b) fragmentation ions confirmed the sequence of the peptide mass at  $m/z$  953 (Fig. S3A).

The ionized mass of peptide P11 [59-LGLNPAIVAGGIPK-72, 1319.8 Da] was found at  $m/z$  660.38 as a doubly charged form, exclusively in fraction 24 (Fig. 3A). Only this fraction was shown to contain SCA2 in a considerable amount (Fig. 2B). This abundance pattern allowed us to assign peptide P11 to the SCA2 sequence. In addition, interpretation of the CID spectrum at  $m/z$  660.38 established the peptide sequence as [LGLNPAIVAGGIPK] by observation of the C-terminal fragmentation ions,  $y_2 - y_{13}$ , and the N-terminal fragmentation ions,  $b_2, b_4, b_6$  and  $b_7$  (Fig. S3B).

In parallel, we ran MALDI-TOF mass spectrometry of each HPLC-SCA from fractions 24, 27 and 30 following trypsin digestion. Besides the major SCA1 tryptic ions, additional ions at  $m/z$  880.5 and 937.5 were observed specifically in the SCA3-abundant fraction 30 (Fig. S4C). ESI-MS/MS analysis of their doubly charged ions at  $m/z$  440.7 and 469.3 (data not shown) indicated that they could be produced from the peptide [KGGVIPPR] where the  $\epsilon$ -NH<sub>2</sub> of the N-terminal K is modified by one or two molecules of iodoacetamide. Indeed, the unmodified (by iodoacetamide) ion at  $m/z$  412.24 was observed only in fraction 30 in ESI-MS, and *de novo* sequencing with observation of the C-terminal

fragmentation ions  $y_1 - y_7$  and one detectable N-terminal ion  $b_5$  indicated that the peptide sequence is [KGGVIPPR] (Fig. S5). The underlined sequence was tightly matched to the new peptide P4 [20-GGVIPPR-26, 695.4 Da] and contained Arg26 (bold letter) instead of Gly26 for SCA1 (Table 1). We assigned peptide P4 to SCA3, because it is specific to the SCA3-enriched fraction in Figure 2D.

*The primary sequence for SCA3 protein is determined, but the total sequence of SCA2 is yet to be identified.*

Through proteomic approaches, we identified two amino acid changes in SCA3 compared to SCA1: Arg26 and Ala71. With these variations, a tentative primary sequence of SCA3 was reconstructed, and its theoretical mass was calculated and compared with the experimental mass from the ESI-MS analysis (Table 2). The theoretical mass of SCA1 with four disulfide bonds shows an identical match with its experimental mass. Likewise, for the SCA3 sequence, its calculated mass was identical to the experimental mass, confirming the total sequence of SCA3.

We identified only one peptide fragment (P11 in Table 1) specific to SCA2. The P11 [59-LGLNPAIVAGG**IPK**-72, 1319.8 Da] contains Pro63 and 69-GIP-71 (bold letters), compared to Ala63 and 69-IPG-71 in SCA1. The P11 was generated in a smaller size than its counterpart from SCA1, P10 [53-SLVNPSLGLNAAIVAGIPGK-72, 1891.1 Da], probably due to an enzyme cut at the location next to Leu59 (underlined). This led us to assume that there is Lys58 or Arg58 in SCA2, but not Ser58, as is the case in SCA1. When amino acid variations found in P11 were applied to the SCA2 primary sequence, neither SCA2<sup>K58</sup> (tentative SCA2 containing Lys58) nor SCA2<sup>R58</sup> (tentative SCA2 containing Arg58) showed a clear match between theoretical and experimental masses (Table 2), indicating that there are more amino acid variations yet to be identified.

*SCA has the conserved sequence and structural motifs found in the plant nsLTP family.*

The primary sequences of SCA isoforms were compared with several plant nsLTPs that show at least 38 % amino acid identity to SCA (Fig. 4).

Eight cysteine residues, four alpha helices, three loops, and a long C-terminal tail appear to be conserved in lily SCAs. Two consensus pentapeptides conserved in plant nsLTPs are found in SCA1 and SCA3: Thr/Ser-X1-X2-Asp-Arg/Lys, 40-44; Pro-Tyr-X-Ile-Ser, 78-82 (50). Among several amino acid residues conserved in plant nsLTPs, two-conserved tyrosine residues located in both N- and C-termini (Tyr16 and Tyr79 in SCA numbering) are also found in SCA. All amino acid variations identified in SCA isoforms are found in relatively non-conserved regions of the nsLTP molecules.

*SCA3 has a different structure from SCA1.*

Based upon the newly identified peptide sequences, the three-dimensional homology structures of SCA proteins were constructed using several plant nsLTP structures as templates (see materials and methods). The structural homology and molecular dynamics modeling showed that SCA1 and SCA3 have structures similar to that of the plant nsLTP family: a globular shape of the orthogonal 4-helix bundle architecture (Tables S1 and S2), four disulfide bonds, a hydrophobic core, a hydrophobic cavity, three loops and a long C-terminal tail in random coil conformation. The disulfide bond patterns of both SCA1 and 3 are identical to each other: Cys3–Cys50, Cys13–Cys27, Cys28–Cys73, and Cys48–Cys87 (Fig. S6). Four disulfide bonds stabilize the whole structure together with the hydrophobic core and their cysteine pairings have the pattern of the type1 plant nsLTP (C<sup>1st</sup>–C<sup>6th</sup> and C<sup>5th</sup>–C<sup>8th</sup>) (10,51,52).

However, SCA3's helices appear to be more tightly packed, compared to SCA1 (Fig. 5, A and B). A superimposition of SCA3 structure on SCA1 highlights several structural changes (Fig. S8): 1) the C-terminal tail of SCA3 falls toward the protein core. 2) The N-terminus and the C-terminal end of the helix H2, and 3) the loops L1 and L3 are positioned closer to each other in SCA3, compared to SCA1. The change from Gly71 in SCA1 to Ala71 in SCA3 is not considered to affect this structural change. They both are small amino acid residues with similar molecular weights (Gly, 57.05 Da; Ala, 71.09 Da). However, Arg26 in SCA3 replacing Gly26 in SCA1 results in formation of a strong hydrogen bond and a strong salt bridge with Asp9 (Fig. 5, C

and D). The calculated distances between the following Asp9-Arg26  $O^{\delta 1}-H^{\epsilon}$ ,  $O^{\delta 2}-H^{\epsilon}$ ,  $O^{\delta 1}-H^{\eta 21}$ , and  $O^{\delta 2}-H^{\eta 21}$  atoms are 3.0 Å, 2.2 Å, 1.9 Å and 2.2 Å, respectively. These new interactions cause the helix H1 (Ser8 – Arg18) of SCA3 to be partially uncoiled and thereby much shorter than that (Gly4 – Arg18) of SCA1 (Fig. 4 and Table S1). It also slightly effects the length of the helix H2 of SCA3 (Arg26 – Asn36), compared to that (Pro25 – Leu37) of SCA1. In addition, the helices H1 and H2 in SCA3 are repositioned in close proximity, unlike SCA1 (Fig. 5D).

The protein surfaces of SCA1, SCA3, and maize LTP were shown to contain mainly solvent-exposed hydrophilic residues, when colored by percent solvent accessibility (Fig. 6, A, D, and G). Overall, there is no noticeable difference in the patterns of hydrophobicity among the three proteins, all of which contain a core of hydrophobic residues (Fig. 6). We have also examined the effect of the structural change due to the presence of Arg26 in SCA3 on the putative internal cavity of SCA. Figure 6B, E, and H show the internal cavities of the three proteins, colored by percent solvent accessibility, after the molecular surfaces are removed. These panels demonstrate that the internal cavities are almost entirely solvent inaccessible. Figure 6C, F, and I show the internal cavities colored by amino acid type, demonstrating that the internal cavities are formed by mainly hydrophobic amino acids.

The visualized internal hydrophobic cavities showed significant differences in size. SCA1 structure shows that a tunnel-like internal cavity passes through the whole molecule from one end to the other (Fig. 6C). It also has a small cavity with lower hydrophobicity, located between the C-terminal sequence and the loop L2. The internal hydrophobic cavity of SCA1 is lined mainly with hydrophobic amino acid residues: the helix H1 (Leu10, Cys13, and Leu14), the helix H2 (Cys27, Gly30, Val31, Leu34, and Asn35), the helix H3 (Thr41, Arg44, Gln45, Ala47, Cys48, Leu51, Lys52, and Val55), the loop L3 (Leu61 and Ala63), the helix H4 (Val66, Ile69, and Pro70), and the C-terminal tail (Tyr79, Pro80, Ile81, Ser82, Met83, Thr85, and Cys87). Unlike SCA1, SCA3 has two discontinuous small cavities (Fig. 6F). One of them is located in the protein core and the other is positioned toward the area between the helices H1 and H3. A few hydrophobic amino acid residues

contribute to form the hydrophobic cavity of SCA3: the helix H1 (Leu10, Thr11, Cys13, and Leu14), the helix H2 (Cys27 and Val31), the helix H3 (Leu51, Leu54, and Val55), the helix H4 (Val66, Ile69, and Pro70), and the C-tail (Ile81). Maize LTP has a continuous hydrophobic cavity in the protein core, although its size is much smaller than that of SCA1 (Fig. 6I). It is formed by hydrophobic side chains of several amino acid residues: Val7, Ala10, Ile11, Cys14, Val33, Leu36, Leu53, Tyr81, and Leu83. The calculated total protein volumes of homology/MD structures at 200ps are quite similar:  $9862\text{\AA}^3$  for SCA1,  $9956\text{\AA}^3$  for SCA3, and  $9225\text{\AA}^3$  for maize LTP1. The volumes of the internal hydrophobic cavities are fluctuating during the MD simulation. Overall, SCA1 displayed a larger cavity (2.3- to 5.1-fold between 200 and 600ps) than that of SCA3.

*The SCA isoforms differ in their adhesion activities with SCA1 being the most active.*

The HPLC-SCAs from fractions 24, 27, and 30 (Fig. 2) were further evaluated for their activities in lily pollen tube adhesion (Fig. 7), using our *in vitro* adhesion assay as described in materials and methods. The SPs, prior to the HPLC purification of SCA, were used as the positive control in every adhesion assay. The numbers of adhered pollen tubes in the control were around 250 to 350. The negative controls, 1) pectin without any protein and 2) pectin plus Bovine Serum Albumin (BSA), usually had less than 100 pollen tubes adhered. Of the eleven experiments, results from only six assays showed reasonable numbers of adhered pollen tubes in both positive and negative controls. These were used to compare adhesion activities of SCAs from the three fractions. Pollen tube adhesion activity was the highest for HPLC-SCAs from fraction 27 where SCA1 is abundant (Fig. 2C). HPLC-SCAs from fraction 30, in which SCA3 was most and SCA1 the least abundant (Fig. 2D), showed a lower level of adhesion activity, but still significant compared to negative controls (Table S3). HPLC-SCAs from fraction 24, in which SCA2 is present in a significant amount (Fig. 2A), showed no difference in activity from the negative controls (Table S3).

The different levels of adhesion activity between SCA1 and SCA3 do not result from differences in pectin-binding ability.

Our previous data show that lily pistil SCA and pectins form an adhesive matrix for the pollen tube (6,7). We also found that, *in vitro*, SCA binds with pectins through a charge interaction to form this adhesive matrix and that this interaction was found to be indispensable for pollen tubes adhering onto the SCA-pectin matrix (6). To examine if this aspect could contribute to different levels of activities between SCA1 and SCA3 in the adhesion assay, we evaluated their pectin-binding abilities using an *in vitro* binding assay (Fig. 8A). All SCA proteins from the SP positive control and three HPLC-purified fractions containing different SCA isoforms were incubated with pectins and applied to 100-kD cut-off spin-columns. All SCA proteins applied to the assay were tightly bound with pectins and found in the retentates, regardless of the SCA isoform used. When the spin-columns were washed with 1M NaCl, after the retentates were removed, no proteins were found left over in the columns.

To better evaluate their pectin-binding abilities, we measured how much ionic strength was required for SCA1 and SCA3 to be detached from the pectin matrix (Fig. 8B). Equal amounts of proteins from SP28 (SCA1-enriched) and SP31 (SCA3-enriched) were incubated with pectins and applied to the spin-columns. Serial elutions using various concentrations of NaCl (0 to 1000 mM) showed that both SCA1 and SCA3 detached from the pectin matrix at 50mM ionic strength.

We have also calculated the strength and spatial distribution of the electrostatic potentials generated by the charges of SCA1 and SCA3 and their interactions with solvent (Fig. 8C). Both proteins generate predominantly positive electrostatic potential owing to the excess of positive charge. SCA3 possesses stronger positive electrostatic potential than SCA1, because of the presence of Arg26. However, this difference is not enough to discriminate between the abilities of SCA1 and SCA3 to interact with pectin within the resolution of the current pectin binding experiment.

The results indicate that the behaviors of both SCA isoforms are identical in pectin-binding abilities and that different levels of adhesion activities of SCA isoforms cannot be fully

understood by the electrostatic potential interaction between SCA and pectins.

*SCA requires an optimal pH and charge to be involved in lily pollen tube adhesion.*

In our previous study, adhesion activity of the SCA-pectin matrix was significantly decreased when it was prepared in extreme pH conditions (below pH 4 and above pH 9) and SCA lost pectin-binding ability at pH 10 (6). The pH-dependent pectin binding is crucial for adhesion activity of the SCA-pectin matrix. To examine the optimal pH for interaction with pectin, we have calculated the titration curves of the SCA isoforms (Fig. 9, A and B). To determine the pH range of structural integrity and the influence of salt on the stability of the SCA isoforms, we have calculated their stability-pH profiles at two ionic strengths, 0 mM and 50 mM NaCl (Fig. 9, C and D). These calculations account for the pH dependence of the protonation sites of all titratable residues of the proteins.

SCA1 showed a positive charge (+5) at pH 4 – 7 but SCA3 showed a slightly higher positive charge (+6) at pH 4 – 6, owing to the presence of Arg26. Above pH 8 or below pH 4, the total charges of both SCAs significantly decreased to negative or increased to more positive, respectively. SCA1 and SCA3 have similar stability-pH profiles, with optimal ion pair formations between acidic and basic residues at pH range ~4 – 11. At extreme pHs, where titratable residues lose their ion pair partners because of neutralization of acidic residues (low pH) or basic residues (high pH), there is loss of stability, as expected. At 0 mM, both SCA1 and SCA3 exhibit maximum stability towards high pH. This is pH 9.5 for SCA1 and pH 10 for SCA3, the difference being attributed to the Gly26Arg mutation. At 50 mM, SCA1 and SCA3 exhibit nearly a plateau in the pH range 4 – 10.5, within ~1 – 1.5 kcal/mol. Introduction of 50 mM ionic strength slightly destabilizes SCA1 in the pH range ~8 – 11 and SCA3 in the pH range ~9 – 12. This difference is attributed to the addition of Arg26 in SCA3.

The titration curves also depict a rigorous way of calculating the pI value of a protein (marked in Fig. 9, A and B). This is done by taking into account the pK<sub>a</sub> shifts of titratable amino acids within the protein, owing to favorable or

unfavorable Coulombic interactions with all other amino acids in the vicinity or desolvation effects. The calculated pI values using the titration curves are higher than those listed in Table 2. Our calculation shows that the optimal pH for interaction of both SCA isoforms with low-esterified pectin is in the range 4 – 7. This pH range corresponds to maximum charge (+5 – +6), where the proteins maintain optimal stability.

## DISCUSSION

### *Purification and sequence identification of SCA isoforms from the lily stigma*

Plant nonspecific (ns) LTPs are present in a multigene family (53,54). Plant nsLTPs have been classified into two groups: type 1 (LTP1, ~10 kDa) and type 2 (LTP2, ~7 kDa) (10,50). Plant nsLTPs are often purified as several isoforms with very similar sequences (52,55-57). To date, no one has determined any functional properties for the isoforms. In lily, SCA was found in multiple forms in the extracellular matrix (ECM), similar to other plant nsLTPs (26).

In the current study, three SCA isoforms were further separated in serial size-column fractions and more clearly identified in ESI-MS following HPLC. In addition to the original SCA isoform (SCA1, 9370 Da) (7), we identified two other isoforms: SCA2 (9384 Da) and SCA3 (9484 Da). Our peptide-sequencing analysis of the isoforms showed three novel trypsin-digested peptides. Each novel peptide contains only one or a few amino acids that differ from the original SCA1 sequence. All other peptides we recovered, except for these new ones, align with the cDNA-deduced SCA1 sequence of 91 amino acids (7), reflecting the reliability of our sequencing data. Evaluating abundances of new peptides in the three HPLC-SCA fractions, where three SCA isoforms were partially separated, enabled us to assign peptide [53-SLVNPSLGLNAAIVAGIPAK-72] and peptide [59-LGLNPAIVAGGIPK-72] to SCA3 and SCA2, respectively. In addition, MALDI-TOF analysis enabled us to identify a SCA3-specific tryptic ion peak and to assign another peptide [20-GGVIPPR-26] to SCA3.

Two peptides were sufficient to rebuild a total mass for SCA3, indicating that SCA3 has only two amino acids that differ from SCA1: Arg26Gly and Ala71Gly. However, we were not able to fully

reconstruct SCA2 (9384 Da) using sequence variations found in this study. Further sequencing analysis, using various proteolytic enzymes, is needed to establish the sequence for SCA2.

### *Homology/MD Structures of SCA isoforms*

SCA isoforms contain several amino acid residues that are conserved among plant nsLTPs, with relation to lipid complexation. In previous studies of the maize LTP-long chain lipid complex, a hydrogen bond was found between the carboxylate or carbonyl group of the lipid and the hydroxyl of the C-terminal Tyr81 (in maize LTP numbering), stabilizing the protein-lipid complex (11,12,58). The conserved N-terminal Tyr17 (in maize LTP numbering) on the helix H1 is mostly solvent exposed (12) and its role in the lipid complexation is obscure. In the conserved Asp-Arg sequence of maize LTP, three arginine residues (Arg41, Arg46, and Arg47) interact with an anionic phosphate group and an aspartic acid (Asp45) is located in the vicinity of the positive choline moiety of the palmitoyl-lysophosphatidylcholine (12).

In homology/MD structures of SCA isoforms, the side chain of Tyr79 is oriented toward the C-terminal entrance of the internal hydrophobic cavity of SCA, while Tyr16 is found adjacent, on the other side of the entrance, similar to that of maize LTP (Fig. S7). Asp43 and Arg44 (corresponding to Asp45 and Arg46 in maize LTP) are found in the Asp-Arg consensus pentapeptides of SCA isoforms, while Lys39 and Gln45 in SCA1 and SCA3 replaces Arg41 and Arg47 in maize LTP, respectively. They are localized to the area near the loop L2 and close to the C-terminal sequence (Fig. S7).

The mode of lipid binding varies depending on the LTP molecules and the types of lipids. The orientation of palmitic acid inserted in the hydrophobic tunnel of barley LTP is upside-down, compared to the Maize LTP-palmitate complex (59). Wheat LTP can bind two molecules of lysomyristoyl-phosphatidylcholines in an anti-parallel way, showing two open entrances at areas between the C-terminal sequence and the loop L2 (site 1) and between the loop L3 and the end of the helix H1 (site 2) (16). Ace-AMP1, an antimicrobial protein from onion seeds, does not contain a continuous hydrophobic cavity in the core of the protein, nor does it display lipid transfer activity *in*

*in vitro* (23,60,61). This indicates that a proper cavity volume needs to be maintained for plant nsLTPs to bind lipids *in vitro*.

In our structural data, SCA1 is shown to contain a large tunnel-like cavity in the interior, stretching continuously from the C-terminal segment to near the loop L1 between the helices H1 and H2. However, SCA3 shows two discontinuous small cavities in the protein interior. The Arg26 in SCA3 is predicted to form strong hydrogen bonds and salt bridges with Asp9 (~2 Å in distance). The calculated  $pK_a$  value of Asp9 in the SCA1 structure is 1.1 (data not shown), which is dramatically changed from that in the model ( $pK_a$  of Asp, 4.0). This indicates that Asp9 strongly interacts with basic amino acid residues and significantly contributes to SCA1 conformation. This new interaction results in significant conformational changes in SCA3, compared to that of SCA1. 1) The helices H1 and H2 become shorter and are positioned in close proximity. The steric hindrance in this area appears to cause one end of the putative cavity to extend toward the area between the helices H1 and H3, unlike those of SCA1 and maize LTP. This unusual distortion may also be responsible for two divided small cavities in SCA3. 2) An overlay of SCA3 structure on SCA1 shows slight internal conversions toward the protein core near two putative entrances of the hydrophobic cavity: 'Top hatch' between the C-terminal sequence and the loop L2, and 'Bottom opening' between the loops L1 and L3. Almost all LTP-lipid complexation studies suggested that the C-terminal sequence is significant in regulating lipid binding. These structural changes possibly limit an interaction with a ligand as well as the surface area in the core of SCA3. This has yet to be determined.

#### *Insights into the mode of action of SCA in the in vitro pollen tube adhesion assay*

In order to form a functional adhesion matrix in our bioassay, both SCA and pectin must interact with each other (6,7). A charge interaction, rather than a covalent binding, between SCA (a small, basic protein) and low esterified pectins (huge, negatively charged carbohydrates) has been proposed (6). This SCA-pectin interaction is dependent on pH and essential for pollen tube adhesion activity (6). In this previous study, the adhesion activities were high when SCA/pectin

matrices were prepared in a range of pH from 5 to 8. No adhesion activity was seen at the extreme pHs (below 4 or above 9). The binding capability of SCA to pectin was significantly lowered in pH10, compared to pH6, as was the pollen tube adhesion activity. Any failure of SCA in binding the pectin in the extreme pHs can result in loss of adhesion activity of the SCA-pectin matrix. This led us to believe that SCA/pectin binding alone was sufficient for an adhesive matrix and to predict that different activities of SCA isoforms in the current study may be associated with their pectin binding capabilities. However, we did not see any significant measurable difference in the *in vitro* pectin-binding assay using the different SCA isoform-enriched fractions.

We have also performed structural homology modeling followed by molecular dynamics simulations to generate three-dimensional models for SCA1 and SCA3 at atomic resolution. We have used the modeled structures to perform Poisson-Boltzmann electrostatic calculations. The rationale for these calculations is two-fold. First, we examined the role of charge and the generated electrostatic potentials, responsible for the interactions with pectin, by comparing the calculated data with the experimental data. Second, we examined the role of charge in the stability of SCA1 and SCA3 as a function of pH. The results indicate that a change in the electrostatic potential due to two amino acid variations (Arg26Gly and Ala71Gly) in SCA3 may not be significant enough to provide a difference in binding to the pectin. The current computational study also suggests that SCA1 and SCA3 are very similar to each other in binding with pectin in a pH-dependent manner. SCA appears to be relatively stable, in terms of conformation, in pH range from 4 to 10.5. This pH-dependent pattern of protein stability can be understood based upon interactions among amino acid residues that reside in SCA. In low or high pHs, basic or acidic amino acids would have different charges at a neutral pH, because they gain or lose protons. The breakdown of overall charge balance in SCA protein at the extreme pH can result in the unfavorable effect of disrupting ionic interactions or salt bridges, which can lead to an inappropriate conformation of SCA. Therefore, SCAs lose an interaction with the pectin when they are combined in the extreme pHs, because of

reduction or loss of structural content. In fact, the physiological pH of lily pistil tissues is 5.6 and the adhesion activity was shown to be greatest when the matrix was prepared at pH 5 to 6 (6). Although SCA proteins were shown to be stable at pH 9 and 10, in which no interaction was found between SCA and the pectin (6), their positive charges were decreased over pH 8 and were approaching negative when above pH 10. This would unfavorably affect SCA interaction with the negative pectins. At below pH 4, the more positive SCAs appear more favorable to pectin binding, but their stability is significantly disrupted. The current study supports the previous idea of the pH-dependent SCA/pectin interaction. However, both SCA1 and SCA3 showed a similar pH-dependence on charge (+5 for SCA1 and +6 for SCA3) as well as conformational stability (pHs 4 – 10.5).

In recent work from our group, we found that plant mono-ubiquitin (Ub, 8.7 kDa), present in a negligible amount in SPs, enhanced lily pollen tube adhesion activity on a SCA-pectin matrix (27). In the present adhesion assay, activity of HPLC-purified SCA was always lower than that of the SPs, which contains other molecular factors such as chemocyanin (26) and mono-Ub (27). An involvement of any of these in the current assays is unlikely because these molecular factors were excluded through HPLC purification. The Mascot protein database search of trypsin-digested HPLC-SCAs for peptide sequence determination did not give us any sequences from chemocyanin or mono-Ub (data not shown). It appears that the difference in adhesion activity we see between SCA1 and 3 is solely due to their different structures, and not due to their different pectin binding abilities or to any involvement of enhancer molecules.

#### *A role for SCA in lily pollination*

SCA, a nsLTP, is secreted from the lily stigma/style and together with the low esterified

pectin forms an adhesive matrix, providing growing pollen tubes a track for guidance to the ovules (1-4). In our first model for the adhesion mechanism, we proposed that this SCA/pectin matrix in the style allowed SCA to bind to the low esterified pectins on the surface of the pollen tube, providing a link between the pectins of the TTE and the pollen tube wall (1,62) (Fig. 10A).

Recently, our group showed that SCA proteins bind initially at the tip region of *in vitro* growing pollen tubes and are then internalized to the cytoplasm of the tube cell through an endocytotic pathway (27). This is also evident in *in vivo* grown pollen tubes, though some lower amount of binding occurs in the wall back from the tip (27). This is in contrast to the model we proposed initially because low esterified pectins are found mainly on the tube walls back from the tip. Esterified pectins predominate at the newly formed wall at the tip. This form of pectin cannot bind SCA (6). The significance of tip binding and endocytosis of SCA is unclear but it certainly negates our initial model that it acts solely outside as an adhesin between the pollen tube wall and the TTE.

In this study, both SCA1 and SCA3 isoforms are shown to have the plant nsLTP-like structure. SCA has conserved amino acids, two pentapeptide motifs, and the hydrophobic cavity, all of which are responsible for lipid complexation in other plant nsLTPs. Although both SCA isoforms showed identical pectin binding abilities, SCA1, which has a larger hydrophobic cavity than SCA3, displayed enhanced pollen tube adhesion activity. This is suggestive of a novel role of SCA1 in pollen tube adhesion. SCA1 may be able to interact with a specific moiety of pectins from the pollen tube wall. Or, it may specifically bind to the pollen tube tip, be endocytosed, and enhance tube cell growth and therefore adhesion (Fig. 10B).

#### REFERENCES

1. Lord, E. (2000) *Trends Plant Sci* **5**(9), 368-373
2. Lord, E. M. (2001) *Sex Plant Reprod* **14**(1-2), 57-62
3. Lord, E. M., and Russell, S. D. (2002) *Annu Rev Cell Dev Biol* **18**, 81-105
4. Lord, E. M. (2003) *J Exp Bot* **54**(380), 47-54
5. Jauh, G. Y., Eckard, K. J., Nothnagel, E. A., and Lord, E. M. (1997) *Sex Plant Rep* **10**(3), 173-180

6. Mollet, J. C., Park, S. Y., Nothnagel, E. A., and Lord, E. M. (2000) *Plant Cell* **12**(9), 1737-1749
7. Park, S. Y., Jauh, G. Y., Mollet, J. C., Eckard, K. J., Nothnagel, E. A., Walling, L. L., and Lord, E. M. (2000) *Plant Cell* **12**(1), 151-163
8. Park, S. Y., and Lord, E. M. (2003) *Plant Mol Biol* **51**(2), 183-189
9. Kader, J. C. (1996) *Annu Rev Plant Physiol Plant Mol Biol* **47**, 627-654
10. Kader, J. C. (1997) *Trends Plant Sci* **2**(2), 66-70
11. Shin, D. H., Lee, J. Y., Hwang, K. Y., Kim, K. K., and Suh, S. W. (1995) *Structure* **3**(2), 189-199
12. Gomar, J., Petit, M. C., Sodano, P., Sy, D., Marion, D., Kader, J. C., Vovelle, F., and Ptak, M. (1996) *Protein Sci* **5**(4), 565-577
13. Heinemann, B., Andersen, K. V., Nielsen, P. R., Bech, L. M., and Poulsen, F. M. (1996) *Protein Sci* **5**(1), 13-23
14. Zachowski, A., Guerbette, F., Grosbois, M., Jolliot-Croquin, A., and Kader, J. C. (1998) *Eur J Biochem* **257**(2), 443-448
15. Hamilton, J. A. (2004) *Prog Lipid Research* **43**(3), 177-199
16. Charvolin, D., Douliez, J. P., Marion, D., Cohen-Addad, C., and Pebay-Peyroula, E. (1999) *Eur J Biochem* **264**(2), 562-568
17. Douliez, J. P., Michon, T., and Marion, D. (2000) *Biochim Biophys Acta* **1467**(1), 65-72
18. Douliez, J. P., Jegou, S., Pato, C., Molle, D., Tran, V., and Marion, D. (2001) *Eur J Biochem* **268**(2), 384-388
19. Sodano, P., Caille, A., Sy, D., dePerson, G., Marion, D., and Ptak, M. (1997) *FEBS Lett* **416**(2), 130-134
20. Bernhard, W. R., Thoma, S., Botella, J., and Somerville, C. R. (1991) *Plant Physiol* **95**(1), 164-170
21. Thoma, S., Hecht, U., Kippers, A., Botella, J., Devries, S., and Somerville, C. (1994) *Plant Physiol* **105**(1), 35-45
22. Molina, A., and GarciaOlmedo, F. (1997) *Plant J* **12**(3), 669-675
23. Phillippe, B., Cammue, B. P. A., Thevissen, K., Hendriks, M., Eggermont, K., Goderis, I. J., Proost, P., Vandamme, J., Osborn, R. W., Guerbette, F., Kader, J. C., and Broekaert, W. F. (1995) *Plant Physiol* **109**(2), 445-455
24. Maldonado, A. M., Doerner, P., Dixon, R. A., Lamb, C. J., and Cameron, R. K. (2002) *Nature* **419**(6905), 399-403
25. Nieuwland, J., Feron, R., Huisman, B. A. H., Fasolino, A., Hilbers, C. W., Derksen, J., and Mariani, C. (2005) *Plant Cell* **17**(7), 2009-2019
26. Kim, S., Mollet, J. C., Dong, J., Zhang, K. L., Park, S. Y., and Lord, E. M. (2003) *Proc Natl Acad Sci U S A* **100**(26), 16125-16130
27. Kim, S. T., Zhang, K. L., Dong, J., and Lord, E. M. (2006) *Plant Physiol* **142**(4), 1397-1411
28. Dubois, M., Gilles, K. A., Hamilton, J. K., Rebers, P. A., and Smith, F. (1956) *Anal Chem* **28**(3), 350-356
29. Blumenkr.N, and Asboehan.G. (1973) *Anal Biochem* **54**(2), 484-489
30. Dong, J., Kim, S. T., and Lord, E. M. (2005) *Plant Physiol* **138**(2), 778-789
31. Schwede, T., Kopp, J., Guex, N., and Peitsch, M. C. (2003) *Nucleic Acids Res* **31**(13), 3381-3385
32. Berman, H. M., Westbrook, J., Feng, Z., Gilliland, G., Bhat, T. N., Weissig, H., Shindyalov, I. N., and Bourne, P. E. (2000) *Nucleic Acids Res* **28**(1), 235-242
33. Han, G. W., Lee, J. Y., Song, H. K., Chang, C. S., Min, K., Moon, J., Shin, D. H., Kopka, M. L., Sawaya, M. R., Yuan, H. S., Kim, T. D., Choe, J., Lim, D., Moon, H. J., and Suh, S. W. (2001) *J Mol Biol* **308**(2), 263-278
34. Lin, K. F., Liu, Y. N., Hsu, S. T. D., Samuel, D., Cheng, C. S., Bonvin, A., and Lyu, P. C. (2005) *Biochemistry* **44**(15), 5703-5712
35. Da Silva, P., Landon, C., Industri, B., Marais, A., Marion, D., Ponchet, M., and Vovelle, F. (2005) *Proteins* **59**(2), 356-367
36. Petsko, G., and Ringe, D. (2004) *Sinauer/New Science Press, London, UK*

37. Adcock, S. A., and McCammon, J. A. (2006) *Chem Rev* **106**(5), 1589-1615
38. Brooks, B. R., Bruccoleri, R. E., Olafson, B. D., States, D. J., Swaminathan, S., and Karplus, M. (1983) *J Comput Chem* **4**(2), 187-217
39. Dominy, B. N., and Brooks, C. L. (1999) *J Phys Chem* **103**(18), 3765-3773
40. Ryckaert, J. P., Ciccotti, G., and Berendsen, H. J. C. (1977) *J Comput Phys* **23**(3), 327-341
41. Wu, J. Z., and Morikis, D. (2006) *Fluid Phase Equilibria* **241**(1-2), 317-333
42. Madura, J. D., Briggs, J. M., Wade, R. C., Davis, M. E., Luty, B. A., Ilin, A., Antosiewicz, J., Gilson, M. K., Bagheri, B., Scott, L. R., and McCammon, J. A. (1995) *Comput Phys Commun* **91**(1-3), 57-95
43. Antosiewicz, J., McCammon, J. A., and Gilson, M. K. (1996) *Biochemistry* **35**(24), 7819-7833
44. Gilson, M. K. (1993) *Proteins* **15**(3), 266-282
45. Sitkoff, D., BenTal, N., and Honig, B. (1996) *J Phys Chem* **100**(7), 2744-2752
46. Yang, A. S., and Honig, B. (1993) *J Mol Biol* **231**(2), 459-474
47. Guex, N., and Peitsch, M. C. (1997) *Electrophoresis* **18**(15), 2714-2723
48. Koradi, R., Billeter, M., and Wuthrich, K. (1996) *J Mol Graph* **14**(1), 51-&
49. Honig, B., and Nicholls, A. (1995) *Science* **268**(5214), 1144-1149
50. Douliez, J. P., Michon, T., Elmorjani, K., and Marion, D. (2000) *J Cereal Sci* **32**(1), 1-20
51. Douliez, J. P., Pato, C., Rabesona, H., Molle, D., and Marion, D. (2001) *Eur J Biochem* **268**(5), 1400-1403
52. Liu, Y. J., Samuel, D., Lin, C. H., and Lyu, P. C. (2002) *Biochem Biophys Res Commun* **294**(3), 535-540
53. Vignols, F., Lund, G., Pammi, S., Tremousaygue, D., Grellet, F., Kader, J. C., Puigdomenech, P., and Delseny, M. (1994) *Gene* **142**(2), 265-270
54. Arondel, V., Vergnolle, C., Cantrel, C., and Kader, J. C. (2000) *Plant Sci* **157**(1), 1-12
55. Ostergaard, J., Hojrup, P., and Knudsen, J. (1995) *Biochim Biophys Acta* **1254**(2), 169-179
56. Castro, M. S., Gerhardt, I. R., Orru, S., Pucci, P., and Bloch, C. (2003) *J Chromatogr B Analyt Technol Biomed Life Sci* **794**(1), 109-114
57. Capocchi, A., Fontanini, D., Muccilli, V., Cunsolo, V., Saviozzi, F., Saletti, R., Lorenzi, R., Foti, S., and Gallechi, L. (2005) *J Agric Food Chem* **53**(20), 7976-7984
58. Gomar, J., Sodano, P., Sy, D., Shin, D. H., Lee, J. Y., Suh, S. W., Marion, D., Vovelle, F., and Ptak, M. (1998) *Proteins* **31**(2), 160-171
59. Lerche, M. H., and Poulsen, F. H. (1998) *Protein Science* **7**(12), 2490-2498
60. Gomar, J., Sodano, P., Ptak, M., and Vovelle, F. (1997) *Fold Des* **2**(3), 183-192
61. Tassin, S., Broekaert, W. F., Marion, D., Acland, D. P., Ptak, M., Vovelle, F., and Sodano, P. (1998) *Biochemistry* **37**(11), 3623-3637
62. Mollet, J. C., Faugeron, C., and Morvan, H. (2007) *Annu Plant Rev* **25**, 69-90
63. Altschul, S. F., Gish, W., Miller, W., Myers, E. W., and Lipman, D. J. (1990) *J Mol Biol* **215**(3), 403-410
64. Higgins, D., Thompson, J., Gibson, T., Thompson, J. D., Higgins, D. G., and Gibson, T. J. (1994) *Nucleic Acids Res* **22**, 4673-4680
65. Nielsen, H., Engelbrecht, J., Brunak, S., and vonHeijne, G. (1997) *Protein Eng* **10**(1), 1-6

#### FOOTNOTES

This study was supported by the National Science Foundation (grant no. IBM0420445 to E.M.L.) and accomplished in partial fulfillment of a Ph.D. thesis for Keun Chae in the CMDB (Cell, Molecular, and Developmental Biology) Ph.D. program at the University of California, Riverside.

The abbreviations used are: ECM, extracellular matrix; SCA, stigma/style cysteine-rich adhesin; MD, molecular dynamics; nsLTPs, nonspecific lipid transfer proteins; TTE, transmitting tract epidermis; HPLC, high performance liquid chromatography; ESI-MS, electrospray ionization mass spectrometry;

MALDI-TOF, matrix-assisted laser desorption/ionization-time of flight; Q-TOF, quadrupole-time of flight; LC-MS/MS, liquid chromatography/mass spectrometry/mass spectrometry; Ub, ubiquitin; PBS, phosphate buffered saline; BSA, bovine serum albumin; PDB, protein data bank.

## FIGURE LEGENDS

**Fig. 1.** Purification of lily stigma proteins (SPs). (A) Small sized protein (<10 kDa) fractions were prepared by purification steps using ion exchange and size exclusion chromatography (Bio-gel P10): staining is with Pon-S. (B) SCA-enriched fractions, 21 to 32, were identified by polyclonal SCA antibodies raised against HPLC-purified SCAs. (C) Chemocyanin (26) was shown to be separated from SCA by use of polyclonal antibodies against His<sub>6</sub>-chemocyanin (30).

**Fig. 2.** HPLC profile of SPs and ESI-MS profiles of HPLC-SCAs. (A) Each SCA-enriched size-column fraction (Bio-gel P10, shown in figure 1) was further purified through HPLC to obtain pure SCA. The HPLC-peaks corresponding to SCAs were collected for ESI-MS analysis. ESI-MS profiles of HPLC-purified SCAs (B, fraction 24; C, fraction 27; D, fraction 30) showed partial separation of SCA isoforms. (E) Composition of SCA isoforms in the crude protein prep from lily stigma was examined using ESI-MS.

**Fig. 3.** ESI-MS analysis of new SCA peptides. The HPLC-purified size-column fraction 24 (A), 27 (B), and 30 (C) were trypsin-digested and then applied to ESI-MS. Each peptide ion peak shows its abundance in fractions where SCA isoforms were separated. Ion mass at  $m/z$  946.04 is the doubly charged SCA1 peptide [53-SLVNPSLGLNAAIVAGIPGK-72, 1891.10 Da] (Table 1, P10). Ion mass at  $m/z$  953.04 is the doubly charged new SCA peptide [53-SLVNPSLGLNAA IVAGIPAK-72, 1905.12 Da] (Table 1, P9). Ion mass at  $m/z$  660.38 indicates the doubly charged new SCA peptide [60-LGLNPAIVAGGIPK-72, 1319.8 Da] (Table 1, P11).

**Fig. 4.** Amino acid sequence of SCA isoforms and other plant non-specific lipid transfer proteins (nsLTPs). SCA-like nsLTPs were obtained from a BlastP search (63) and aligned using ClustalW (64). Mature protein sequences were generated by prediction of putative cleavage sites of the N-terminal signal peptide using SignalP at the server (<http://www.cbs.dtu.dk/services/SignalP-2.0>) (65). Dashes represent sequence areas that were expanded to allow optimal alignment. Highly conserved amino acids are marked by asterisks. Eight conserved cysteines in the plant nsLTP family are shown as bold asterisks. Four alpha-helices of SCA1 are underlined. Two consensus pentapeptide motifs are shown in boxes: Thr/Ser-X1-X2-Asp-Arg/Lys and Pro-Tyr-X-Ile-Ser. SCA isoform amino acid variations are indicated by bold letters. Protein database accession numbers for plant nsLTPs: Q9SW93, *Lilium longiflorum* SCA1; NP\_181388.1, Arabidopsis LTP1; NP\_181387.1, Arabidopsis LTP2; NP\_568905.1, Arabidopsis LTP3; NP\_568904.1, Arabidopsis LTP4; NP\_190728.1, Arabidopsis LTP5; NP\_187489.1, Arabidopsis LTP6; AF198168\_1, *Aerides japonica* PLTP; O65091, *Oryza sativa* LTP4; Q43766, *Hordeum vulgare* LTP3; Q42848, *Hordeum vulgare* LTP 7a2b; Q42614, *Brassica napus* LTP1; Q42615, *Brassica napus* LTP2; Q42616, *Brassica napus* LTP3; P19656, Maize LTP; Q03461, *Nicotiana tabacum* LTP2.

**Fig. 5.** Ribbon models of two SCA isoforms. Based upon amino acid variations determined by peptide sequencing analysis, three-dimensional structures of SCA1 and SCA3 were generated by homology/MD modeling. (A) SCA1 structure, G71 and G26 are designated in green colored letters. (B) SCA3 structure, A71 (green) and R26 (blue). (C) G26 in SCA1 does not interact with D9. (D) R26 in SCA3 is shown to have strong hydrogen bonding and salt bridge interactions with D9. H1 – H4 indicate helices1 – 4, respectively. L1 – L3 represent loops1 – 3.

**Fig. 6.** The internal hydrophobic and solvent-inaccessible cavities of SCAs. The surfaces of homology/MD structures for SCA1 (A) and SCA3 (D), and a homology/crystal structure for maize LTP (G) are colored by relative percent solvent accessibility. The order of the color code is from hydrophilic

(red) to hydrophobic (blue) amino acids: Red-Orange-Yellow-Green-Cyan-Blue-Dark Blue. Dark blue color indicates completely buried amino acids. Red colored ones are at least 75% solvent exposed. The internal cavities of the proteins are shown after the molecular surfaces are eliminated (B, E, and H). The internal cavities are shown colored by amino acid type (C, F, and I): basic (blue), acidic (red), polar (yellow), and hydrophobic (grey) amino acids.

**Fig. 7.** *In vitro* adhesion assays using HPLC-purified SCA isoforms. (A) The result was obtained from six replicates showing reasonable numbers of pollen tubes adhered on both treatment (250 – 350) and control matrices (~100). SP, pectin matrix prepared with SCA-enriched size-column fractions prior to the HPLC purification as a positive control of adhesion activity; Pectin, pectin matrix alone without any protein (a negative control); BSA, pectin matrix with bovine serum albumin (BSA) replacing SCA (a negative control); HPLC 24 – 30, pectin matrices containing the HPLC-purified SCA proteins from Bio-gel P10 fractions 24, 27, and 30, respectively. (B) All SCA proteins, obtained from the HPLC-purification, were quantified by the Lowry modified protein assay in order to apply equal amounts of proteins for each assay. 5  $\mu$ g of proteins from fractions were also evaluated through Coomassie brilliant blue staining following SDS-PAGE.

**Fig. 8.** Pectin binding abilities and electrostatic potentials of SCAs. (A) HPLC-SCAs (fraction 24, 27 and 30) were applied for the *in vitro* pectin-binding assay. SP, positive protein control prior to HPLC purification; C, 10 $\mu$ l aliquot of protein-pectin mixtures as the loading control; R, Retentate from the 100kDa cut-off spin-column containing proteins bound to pectins; E, Elute containing proteins washed off by 1M NaCl. (B) Ionic strengths needed for detachment from the pectin matrix were measured for SCA1 and SCA3, respectively. SP28 and SP31, Bio-gel P10 size-column fractions 28 (SCA1-enriched) and 31 (SCA3-enriched), respectively; C, The loading control; 0 – 1000 mM NaCl, Elutes containing proteins that were serially washed off using a gradient of ionic strengths; L, Retentate containing proteins that were left over in the spin-column after the final elution using 1M NaCl. (C) Electrostatic potentials for homology/MD structures of SCA1 and SCA3. Iso-potential contour plots at  $\pm 1$   $k_B T/e$  for both SCA1 and SCA3 were generated using GRASP at 0 and 50mM ionic strengths. Blue indicates a positive and red a negative electrostatic potential.

**Fig. 9.** The titration curves and the pH dependence of charges and relative stabilities for the two SCA isoforms. Homology/MD structures of SCA1 and SCA3 were used to calculate the titration curves (A and B) and the pH-effect on protein stability (C and D). The charge values represent the protein net mean charges at every pH value. The calculated isoelectric points, using the apparent  $pK_a$  calculation method, are marked in the titration curves. The stability represents the difference in the ionization free energy of the folded and unfolded protein states. A lower free energy value indicates higher stability.

**Fig. 10.** A model for SCA's roles in lily pollination. (A) A role as an adhesin. Both SCA isoforms play a role in binding a site in the low-esterified pectins from both the ECM of the lily stigma/stylar TTE and the tube cell wall back from the tip. A charge interaction between positive SCAs and the negative low-esterified pectin is indispensable for this pollen tube adhesion event but a more specific interaction of SCA with a carbohydrate moiety in the pectin may be occurring, making SCA a lectin-like protein. (B) Our current study on structural features and activity of SCA isoforms suggests a putative novel role of SCA, regardless of pectin binding, in pollen tube adhesion. Tube cell tip binding and endocytosis may be SCA isoform-specific. The larger hydrophobic cavity may make SCA1 more efficient than SCA3 in these processes, enhancing pollen tube growth and therefore the adhesion event.

Table 1. Amino acid sequences of peptides analyzed by nano-ESI-MS-MS from tryptic digestion of HPLC-purified SCA isoform peaks.

Peptides (AA No.)	Sequence of Analyzed Peptides	Theoretical Mass # (Da)	Experimental Mass ## (Da)
P1 (1 - 18)	I(L)TC*GQVSDSL(I)TSC*L(I)GYAR	2015.9	2015.9
P2 (19-32)	KGGVI(L)PPGC*C*AGVR	1427.7	1427.7
P3 (20-32)	GGVI(L)PPGC*C*AGVR	1299.6	1299.5
P4 (20-26)	<u>GGVI(L)PPR</u>	695.4	695.4
P5 (27-32)	C*C*AGVR	722.3	ND
P6 (33-39)	TL(I)NNL(I)AK	773.5	773.5
P7 (40-44)	TTPDR	589.3	ND
P8 (45-52)	QTAC*NC*L(I)K	994.4	994.4
P9 (53-72)	<u>SL(I)VNPSL(I)GL(I)NAAI(L)VAGI(L)PAK</u>	1905.1	1905.1
P10 (53-72)	SL(I)VNPSL(I)GL(I)NAAI(L)VAGI(L)PGK	1891.1	1891.2
P11 (60-72)	<u>L(I)GL(I)NPAI(L)VAGGI(L)PK</u>	1319.8	1319.8
P12 (73-89)	C*GVNI(L)PYPI(L)SMQTDC*NK	1996.9	1996.9
	C*GVNI(L)PYPI(L)SmQTDC*NK	2012.9	2012.9
P13 (73-91)	C*GVNI(L)PYPI(L)SMQTDC*NKVR	2252.1	2252.1
	C*GVNI(L)PYPI(L)SmQTDC*NKVR	2268.1	2267.9
P14 (89-91)	VR	274.2	ND

Theoretical masses (#) were calculated with the cysteine residues modified by carboxyamidomethylation using ExPASy (Expert Protein Analysis System) server at <http://us.expasy.org>; Experimental masses (##) were expressed, when applicable, as the mean  $\pm$  standard deviation of the masses obtained from analysis of identical peptides; \*, Conserved cysteine residues; M, methionine and m, methionine oxidized as MSO (methionine sulfoxide); ND, Not determined; Underline indicates the newly identified peptides, which contain some amino acid variations from SCA1; Bold letters indicate amino acids within a peptide which differ from SCA1.

Table 2. Comparison of theoretical mass data calculated based upon tentative amino acid sequences and experimental SCA isoform masses from ESI-MS analysis.

Isoform	pI*	pI <sup>¶</sup>	Theoretical Mass (Da) <sup>#</sup>		Experimental Mass (Da)**
			No S-S bond	Four S-S bonds	
SCA1	8.90	11.1	9378.94	9370.94	9369.8 ± 1.0
SCA2 <sup>R58</sup>	9.06	–	9474.09	9466.09	9383.6 ± 1.3
SCA2 <sup>K58</sup>	9.05	–	9446.07	9438.07	9383.6 ± 1.3
SCA3	9.06	11.3	9492.10	9484.10	9483.4 ± 1.1

Theoretical masses (#) and pI values (\*) were calculated using ExPASy (Expert Protein Analysis System) server at <http://us.expasy.org>. pI values of SCA isoform structures were also calculated using computational modeling (¶). Experimental masses (\*\*) were obtained without reduction of the cysteine residues. SCA2<sup>R58</sup> or SCA2<sup>K58</sup> indicate a tentative SCA2 sequence containing Arg58 or Lys58, respectively.

# Figure 1

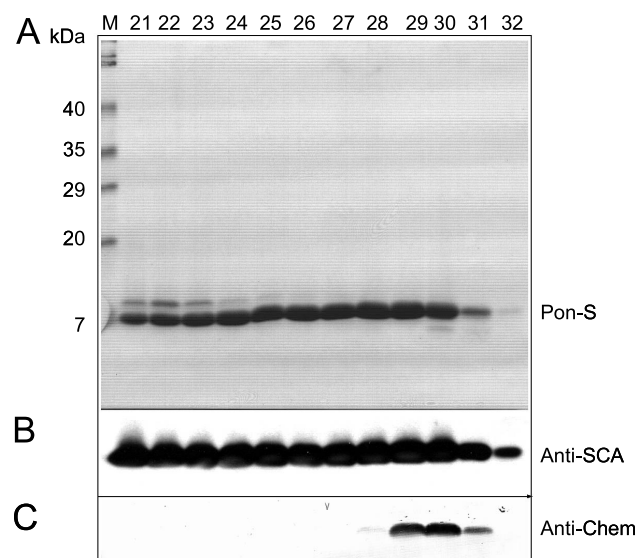


Figure 2

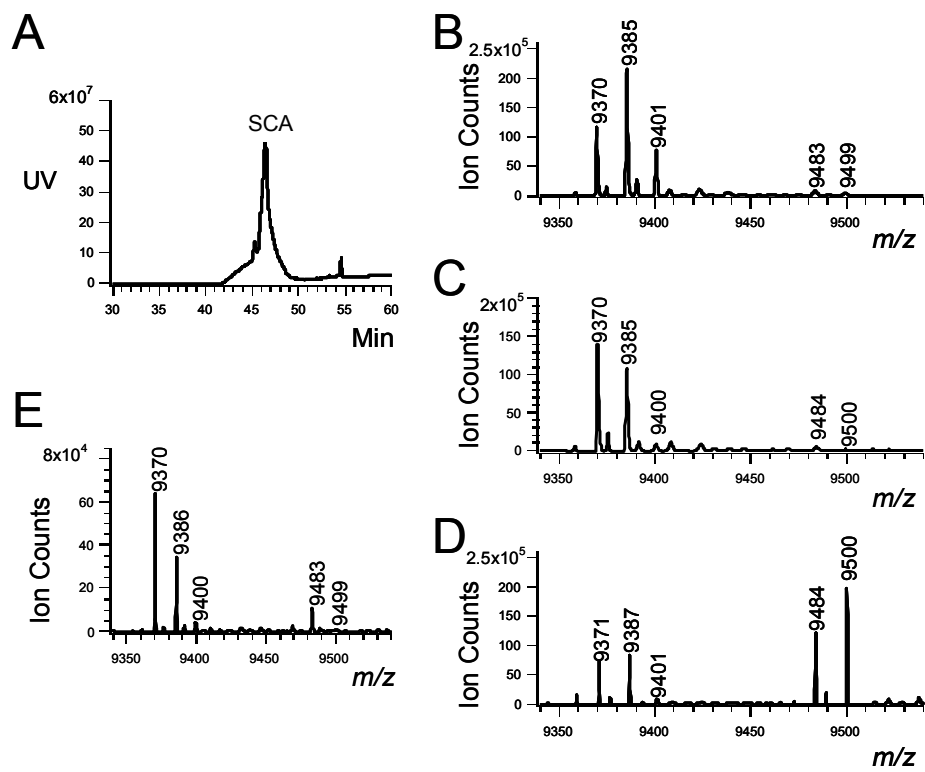


Figure 3

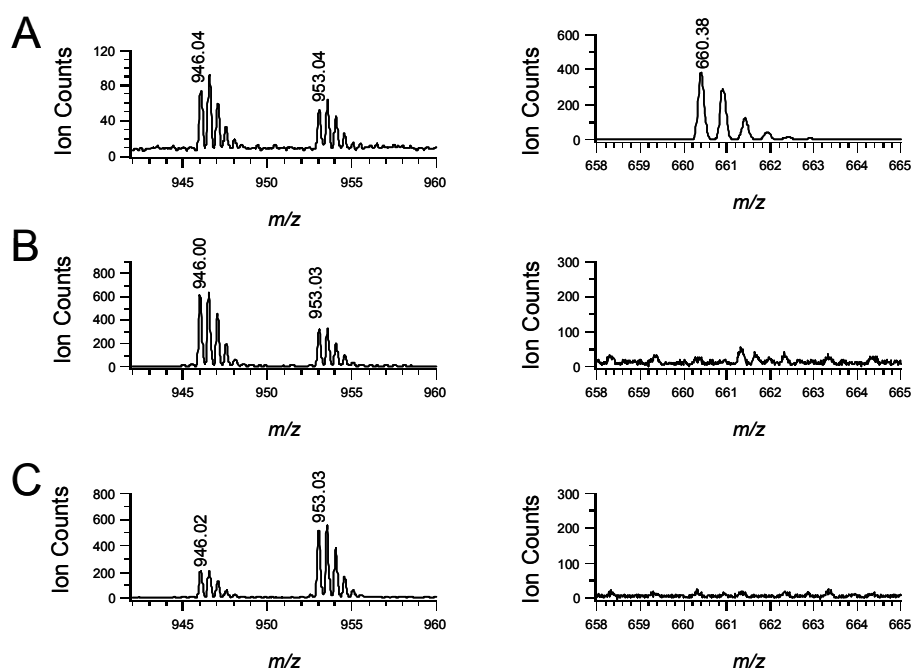




Figure 5

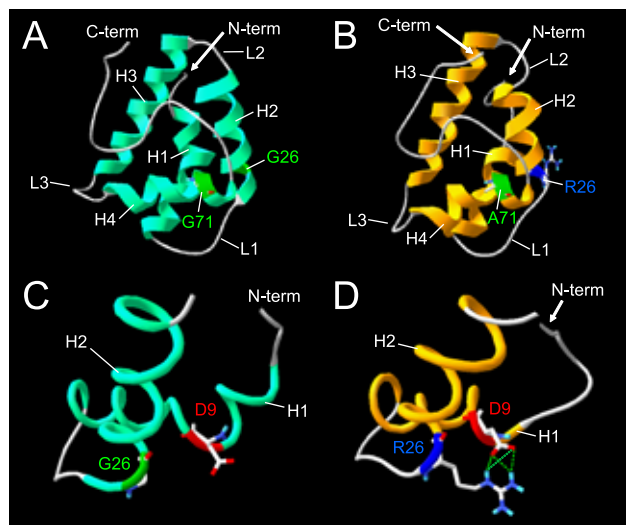


Figure 6

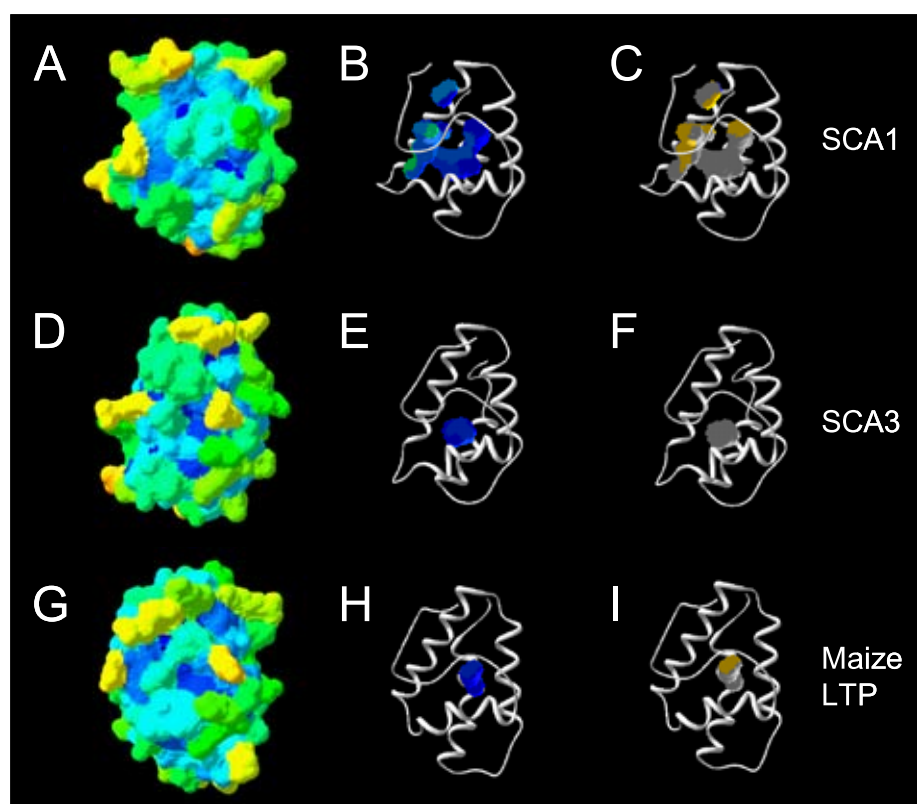


Figure 7

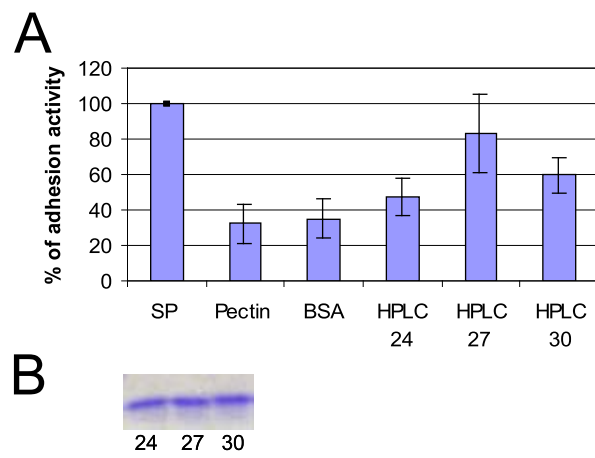


Figure 8

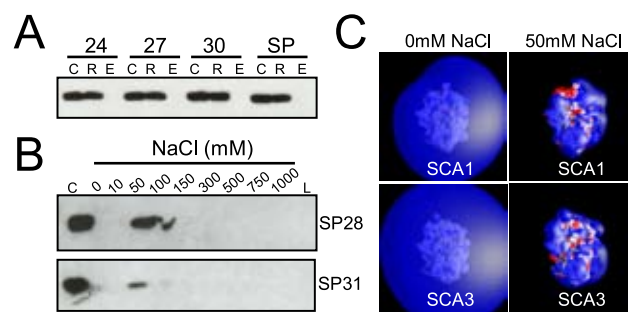


Figure 9

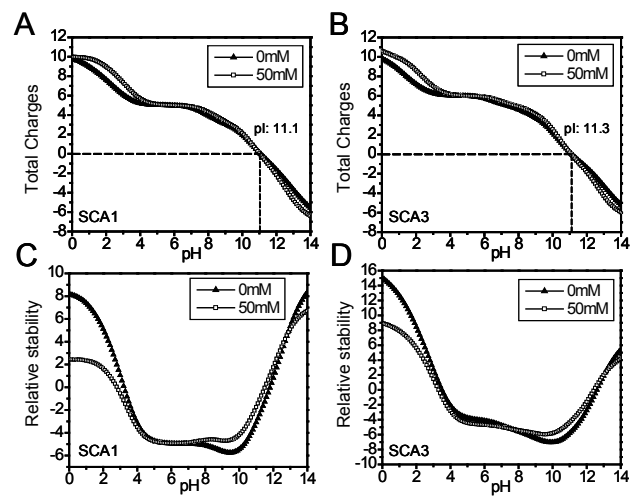


Figure 10

